c.3G>A mutation in the *CRYAB* gene that causes fatal infantile hypertonic myofibrillar myopathy in the Chinese population

Xin-Guo Lu[1,2], Uet Yu[2], Chun-Xi Han[1,2,*], Jia-Hui Mai[2], Jian-Xiang Liao[2], Yan-Qi Hou[3]

[1] *Department of Neuromuscular Research Lab, Shenzhen Children's Hospital, 518038 Shenzhen, P. R. China*

[2] *Department of Neurology, Shenzhen Children's Hospital, 518038 Shenzhen, P. R. China*

[3] *Running Gene Inc.,100083 Beijing, P. R. China*

*Correspondence: hanchunxi60@163.com (Chun-Xi Han)

Infantile hypertonic myofibrillar myopathy is characterized by the rapid development of rigid muscles and respiratory insufficiency soon after birth, with very high mortality. It is extremely rare, and only a few cases having been reported until now. Here we report four Chinese infants with fatal neuromuscular disorders characterized by abdominal and trunk skeletal muscle stiffness and rapid respiratory insufficiency progression. Electromyograms showed increased insertion activities and profuse fibrillation potentials with complex repetitive discharges. Immunohistochemistry staining of muscle biopsies showed accumulations of desmin in the myocytes. Powdery Z-bands with dense granules across sarcomeres were observed in muscle fibers using electron microscopy. All patients carry a homozygous c.3G>A mutation in the *CRYAB* gene, which resulted in the loss of the initiating methionine and the absence of protein. This study's findings help further understand the disease and highlight a founder mutation in the Chinese population.

Keywords

Myofibrillar myopathy; Infant; Neuromuscular disease; *CRYAB* mutation

1. Introduction

Infantile hypertonic myofibrillar myopathy (MFM) causes the rapid development of rigid muscles, respiratory insufficiency soon after birth, loss of myelinated fibers and the presence of giant axons with thin myelin sheets [1]. It was first reported in several Canadian patients and was predicted to be transmitted by autosomal recessive inheritance [2].

Del Bigio *et al.* [1] analyzed the DNA of eight Canadian patients with infantile hypertonic MFM. They observed a homozygous deletion c.60delC in the alpha B-crystallin (αBC) expressing gene, *CRYAB*, in all patients. The mutation led to the loss of αBC expression in muscle fibers. It resulted in patients' pathological features, including endomysial fibrosis, different sizes of myofiber, homogeneous eosinophilic inclusions and peculiar powdery, granular transformation Z-bands [2]. It has also been demonstrated that heterozygous mutations of *CRYAB* (different from *CRYAB* mutations identified in infantile hypertonic MFM) are the cause of MFM2, a specific form of MFM [3–5]. MFM2 occurs at middle age (an

average age ranged from 35 years to 45 years) and is characterized by distinct clinical features compared to the infantile hypertonic MFM [5–7].

Patients with MFM2 typically develop proximal and distal limb muscle weakness associated with neck, trunk and palatopharyngeal muscle involvement, pulmonary insufficiency associated with paresis of the diaphragm, weakness of the cervical, cardiomyopathy and cataracts can be associated features sometimes [5]. So far, about 19 heterozygous *CRYAB* mutations have been described in association with MFM2 [3, 4, 8–19]. However, the infantile hypertonic MFM caused by homozygous *CRYAB* mutations is extremely rare. Since the first description c.60delC in 2011, only other two *CRYAB* mutations have been reported, including a female Caucasian infant with the homozygous mutation c.343delT and a male Chinese infant with the homozygous mutation, c.3G>A [20, 21]. We need more cases to further identify and understand the disease as well as improve the diagnosis.

This case report described infantile hypertonic MFM characteristics in four Chinese infants who developed the disease shortly after birth. The same homozygous mutation, c.3G>A in the *CRYAB* gene, was identified in all patients. This may be a critical hotspot mutation that contributes to the disease's pathogenesis in Chinese infants.

2. Methods

2.1 Clinical data acquisition

Clinical information of all four patients was collected with written consent from their parents (Table 1). Parents of all four patients are non-consanguineous. Patients 2 and 3 have no siblings, while patient 1 has two sisters, and patient 4 has a brother, whose phenotypes were normal.

Laboratory assessments were performed, including complete blood count, serological evaluations of liver, kidney, and heart functions. Electrocardiogram, echocardiography, electromyograms, and magnetic resonance imaging (MRI) were also applied.

Table 1. Clinical data of patients.

Patient	Age at onset (Age at diagnosis)	Presentation	Clinical course	Laboratory assessments	Outcome	Family Structure (siblings)
1	6 months (8 months)	Feeding difficulty, pale skin, paroxysmal irritability	Rapid progressive muscle rigidity, breathing insufficiency, severe pneumonia, and required continued ventilation	CK: 1838 IU/L (24-229 IU/L) CKMB: 533.4 ng/mL (0-6.8ng/mL) ALT: 49 IU/L (0-40 IU/L) AST: 99 IU/L (0-40 IU/L)	Died at 12 months	Two phenotypically normal sisters
2	3 months (5 months)	Feeding difficulty, cyanosed, respiratory distress, tachypnea	Rapid progressive rigidity of neck and trunk muscles, breathing insufficiency, severe pneumonia, and required continued ventilation	CK: 789 IU/L (24-229 IU/L) CKMB: 291 ng/mL (0-6.8ng/mL) ALT: 34 IU/L (0-40 IU/L) AST: 61 IU/L (0-40 IU/L)	Died at 10 months	No
3	8 months (13 months)	Muscle stiffness in the neck, respiratory distress	A slow progression of the rigidity of neck, chest, and abdominal muscles, sudden breathing insufficiency, pneumonia, alive on continued ventilation	CK: 442 IU/L (24-229 IU/L) CKMB: 109 ng/mL (0-6.8ng/mL) ALT: 18 IU/L (0-40 IU/L) AST: 48 IU/L (0-40 IU/L)	Remained on mechanic ventilation at home	No
4	3 months (5 months)	Progressive rigidity, immobility of neck and trunk	A slow progression of muscle rigidity, immobility of neck and trunk, weakness of limbs, respiratory infections, alive on continued ventilation	CK: 1680 IU/L (24-229 IU/L) CKMB: 310 ng/mL (0-6.8ng/mL) ALT: 87 IU/L (0-40 IU/L) AST: 83 IU/L (0-40 IU/L)	Died at 15 months	One phenotypically normal brother

Abbreviations are as follows: CK, creatine kinase; CKMB, creatine kinase myocardial bound; ALT, alanine aminotransferase; AST, aspartate aminotransferase.

2.2 Histopathological and immunochemical analysis

The *vastus lateralis* of patient 2 (four months and 20 days old), rectus abdominis of patients 3 and 4 (six months old) were obtained and processed for the following analysis. For histopathological analysis, muscle specimens were fixed in 10% formalin, embedded in paraffin, prepared into 10 μm sections, then routinely stained with Hematoxylin & Eosin (HE) and Modified Gomori trichrome (MGT). For immunohistochemistry (IHC) staining, muscle specimens were cryopreserved in liquid nitrogen immediately after biopsies. Tissue blocks were cut into 8 μm cryosections and then stained against desmin (Desmin Monoclonal Antibody, 10H7D2). For electron microscopy, muscle tissues were fixed in 2.5% glutaraldehyde, postfixed in 1% osmic acid, dehydrated, and embedded in resin. Ultrathin sections were stained with 2% uranyl acetate followed by lead citrate and examined with JEM-1400 PLUS Transmission electron microscope.

It should be mentioned that patients 3 and 4 were at the same age when the experiments were performed. The results of the experiments were almost the same. Thus, only biopsy findings of patients 2 and 4 have been chosen to be analyzed.

2.3 Genetic analysis

Proband's DNA was sequenced to discover the causal genes. DNA was isolated from peripheral blood with CWE9600 Automated Nucleic Acid Extraction System using CWE2100 Blood DNA Kit V2 (CWBiotech, P. R. China, CW2553). 750 ng genomic DNA was fragmented into 200-300 bp length by Scientz08-III Ultrasonic Homogenizer (SCIENTZ, P. R. China). End-repairing, A-tailing, and adaptor ligation procedures were then processed on the DNA fragments using the KAPA Library Preparation Kit (Illumina, KR0453, v3.13), followed by an 8-cycle pre-capture PCR amplification. Then, the amplified DNA sample was captured in the Agilent SureSelect XT2 Target Enrichment System (Agilent Technologies, Inc., USA). Captured DNA fragments were purified by Dynabeads MyOne Streptavidin T1 (Invitrogen, Thermo Fisher Scientific, USA) and amplified by 13-cycle post-capture PCR. The final products were purified by Agencourt AMPure XP (Beckman Coulter, Inc., USA) and quantitated with Life Invitrogen Qubit 3.0 by Qubit dsDNA HS Assay Kit (Invitrogen, Thermo Fisher Scientific, USA). Eventually, quantified DNA was sequenced with 150-bp paired-end reads on the Illumina Novaseq 6000 platform (Illumina, Inc., USA) according to the standard manual.

The raw data produced by the Novaseq platform were filtered and aligned against the human reference genome (hg19) using the BWA Aligner (http://bio-bwa.sourceforge.net/) after being evaluated according to Illumina Sequence Control Software. The single-nucleotide polymorphisms were called by GATK software (Genome Analysis ToolKit) (www.broadinstitute.org/gatk). Variants were annotated using ANNO-VAR (annovar.openbioinformatics.org/en/latest/). The effects of single-nucleotide variants were predicted by SIFT, Polyphen-2, and MutationTaster programs. All variants were interpreted according to ACMG standards [22] and categorized as pathogenic, likely pathogenic, variants of unknown clinical significance (VUS), likely benign and benign.

3. Results

3.1 Clinical presentation

Patients reported in this study were male, aged from 3 months to 8 months at the onset time of disease. They all had stubby necks and felt unusually hot and sweaty. Physical examination during admission revealed that the four patients displayed a rigid neck, trunk, and abdomen. We observed mild proximal muscle weakness in their extremities, while their limbs' distal muscles seemed familiar. The patients did not display any pathological reflexes, except patient 3, who showed a loss of superficial and deep tendon reflexes. All patients developed an early and severe rigidity in *rectus abdominis*, neck muscles, intercostal muscles, and trunk muscles, causing early respiratory dyskinesia and irreversible respiratory failure, later associated with secondary respiratory infections (Fig. 1). Patients 1 and 2 experienced significant feeding difficulties, which caused mild malnutrition symptoms. Additionally, three of four patients presented several distinctive features during the initial visit to the hospital. Patient 1 presented with pale skin and paroxysmal irritability, which resemble the symptoms of anemia. Patient 2 showed cyanosis after crying, which was suspected to be hypoxemia. Patient 3 displayed increased flexibility of the limbs accompanied by constant hand waving and leg lifting. The clinical characteristics are listed in Table 1.

Laboratory assessments were also performed. The levels of serum creatine kinase (CK), creatine kinase myocardial bound (CKMB), alanine aminotransferase (ALT), and aspartate aminotransferase (AST) were higher for all patients compared to normal people (Table 1). Patients 2 and 4 showed an increase in anti-Acetylcholine (Ach) receptor antibodies in the serum. We treated patient 2 with dexamethasone (1 mg/kg/day) using intravenous drip therapy for a week, while there were no effects. We performed blood and urine test to screen for congenital metabolic diseases, and none were identified. The analysis of cerebral spinal fluid was performed on patients 1 and 3, and the results were normal. All patients developed pneumonia at different degrees. This was confirmed by a computed tomography chest scan or chest x-ray. The electrocardiogram examination of patient 3 indicated enlargement of the right ventricular. Echocardiography analyses suggested that the cardiac functions of all patients remained normal at the time of hospitalization.

Medical histories of all patients were reviewed to exclude neuromuscular damages caused by subclinical infections or trauma. Patient 1 was suspected of experiencing a regression in his motor function a few days before the symptoms occurred. Since then, he has required assistance to sit still. Patient 2 was not able to raise his head at the age of 3 months. We observed abdominal lumps in the back of the right neck and left waist in patient 1 for two months and patient 3 for
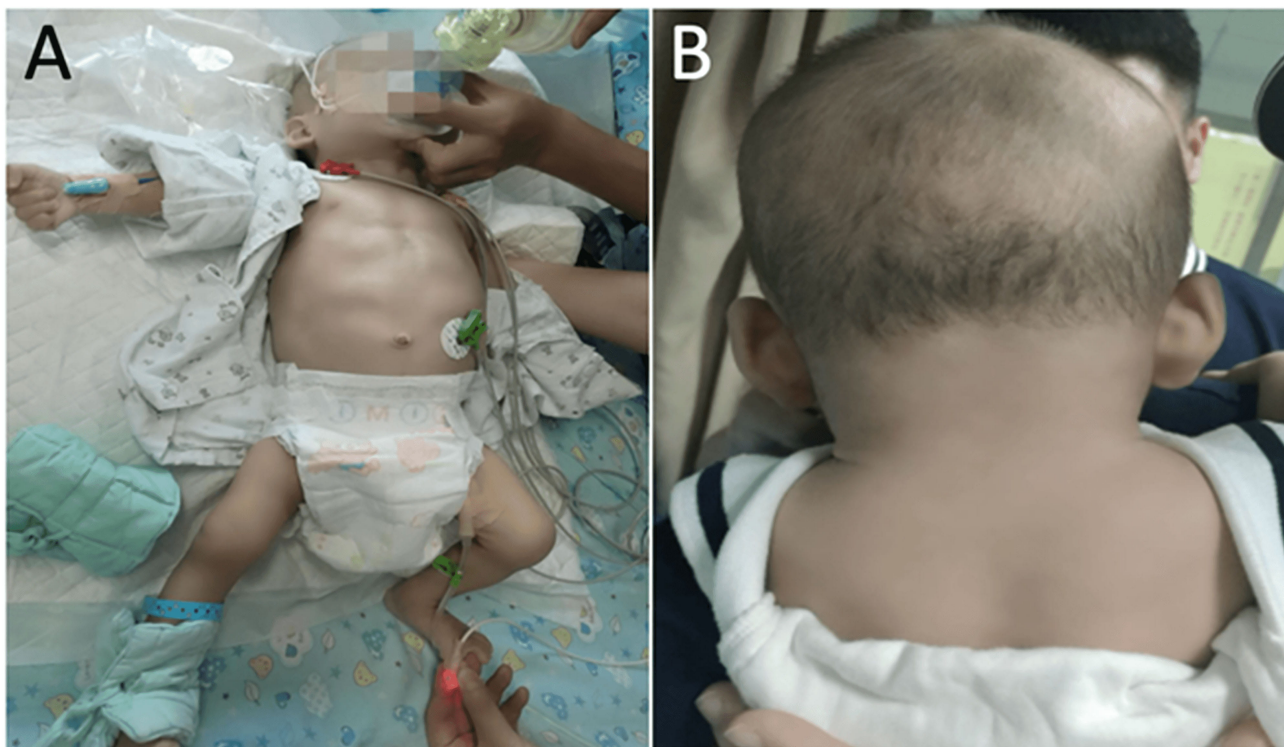
Fig. 1. Clinical photos of patient 3. (A) The patient has a firm texture in the stiff abdominis muscle, which looks like the abdominal muscles of bodybuilders and protrudes. (B) The neck and shoulders are webbed and connected, muscles of which are stiff.

seven months before admission, caused by a hyper-muscular contraction. However, neither of them received appropriate medical treatment before the sudden aggravation of the disease. We did not observe any suspicious incentives except for patient 1, who received an influenza vaccination three days before the disease onset. The patients did not have dysmorphic features or a family history of similar diseases, including neuropathy or neuromuscular diseases. All patients eventually developed severe respiratory distress and hypoxia, requiring ventilation.

The patients were given symptomatic supportive treatment after admission, including increasing nutrients in the muscles, improving gastrointestinal function, anti-infection medications, and ventilator-assisted breathing. However, we failed to prevent the progression of muscle rigidity and cardiorespiratory dysfunction. Patients 1, 2, and 4 died at 12 months, 10 months, and 15 months, respectively. Patient 3 remained alive but required the assistance of mechanical ventilation.

3.2 Magnetic resonance imaging (MRI)

MRI showed similar neuromuscular abnormalities in patients 1 and 3. We observed high-intensity T2WI (T2-weighted images) signals in the *rectus abdominis*, the spinal cord, and the bladder. We also noticed the thickening of *erector spinae fascia* on both sides. Short time inversion recovery (STIR) showed a high signal of damaged waist muscles and rectus abdominis, while the T1WI (T1-weighted images)

channel scan displayed a low overall signal (Fig. 2). T2WI and T1WI are two basic MRI images, highlighting fat and water, fat tissues within the body, respectively. The contrast between these two image types makes doctors diagnose issues with soft tissues. MRI results described above indicated early mild fat infiltration and severe edema in skeletal muscles such as the intercostal muscles and the rectus abdominis. These characteristics are positively associated with irreversible respiratory movement disorders and respiratory failure during infancy. The MRI examinations of the other two patients showed no neuromuscular abnormalities. We performed electromyogram (EMG) in patients 1 and 2, and the results presented similar complex repetitive discharges (CRD) without waveform of myotonic discharge (Fig. 3). Also, we observed an increase in insertion activities and profuse fibrillation potentials when we stimulated the right rectus abdominis muscle of patient 1 and the iliopsoas and deltoid muscles of patient 2.

3.3 Histological examinations

We performed the histopathological and immunohistochemical examinations of muscle biopsies obtained from patients 2 and 4 (Fig. 4). Compared to the specimen collected from the unaffected limb, *rectus abdominis* muscle biopsies showed irregular muscle fibers and significant changes in myocytes with regeneration. IHC staining showed an accumulation of desmin within the myocytes. Electron microscopy (EM) results showed dense granules in the Z-bands and sar-
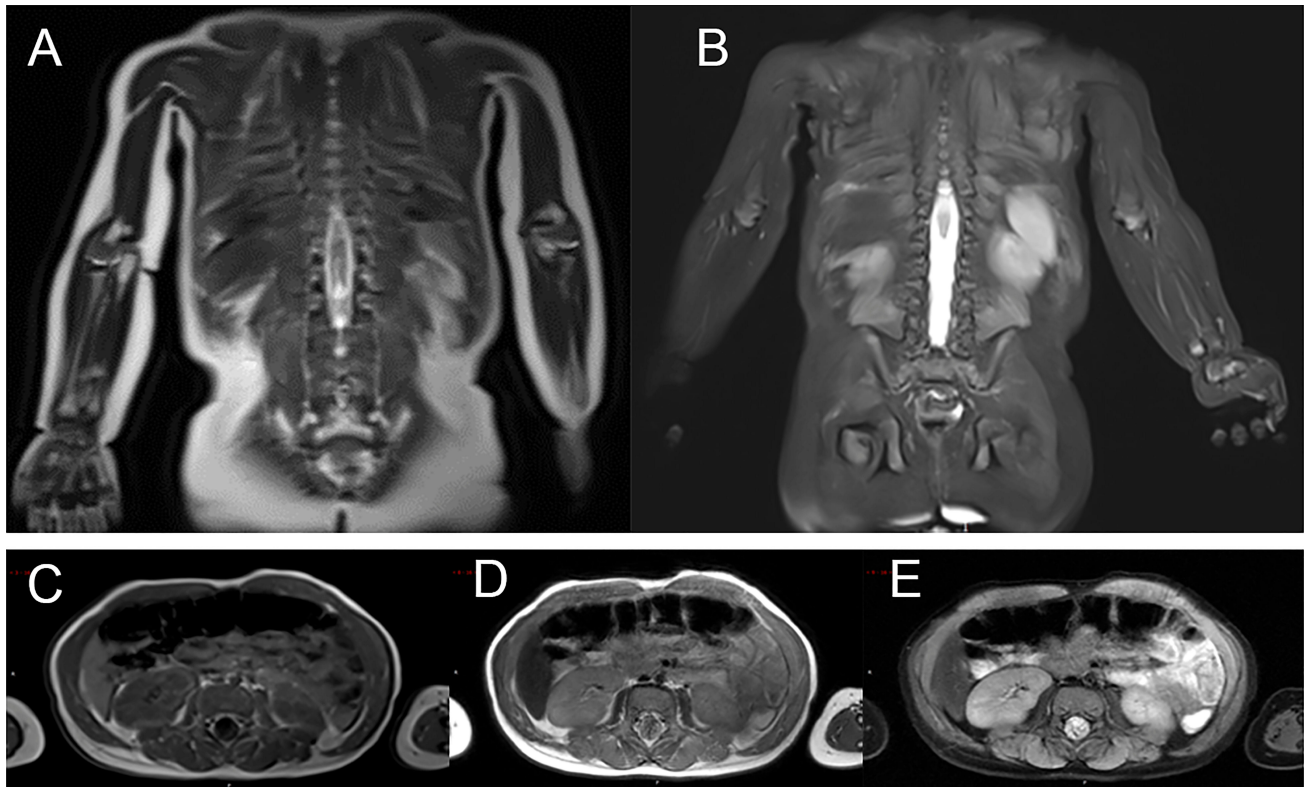
Fig. 2. Muscle MRI of patient 3. (A) T2WI coronal body scan showed a high signal in the waist erector spinae fascia muscle, spinal cord, and bladder area. No abnormalities were identified in the muscles of the limbs. (B) STIR coronal body scan showed a visible high signal in the damaged waist muscles, which is different from the high signal of the spinal cord's cerebrospinal fluid. This result suggests the presence of waist muscle edema. (C) T1WI transverse abdominal scan showed a low signal. Both T2WI transverse abdominal scan (D) and STIR transverse abdominal scan (E) showed a significantly high signal in the rectus abdominis, indicating the muscle edema in the rectus abdominis.

comeres within the muscle fibers. These results were consistent with ultramicroscopic myogenic damage and pathological changes in the muscular biopsy, enabling the present disease classification as an MFM. However, we could only analyze a small number of patient tissues. It is possible that a broader sampling could reveal additional pathological changes at the emerging level.

3.4 Genetic analysis

Genetic sequencing was performed. We detected the homozygotic mutation c.3G>A in the α-B crystal protein gene *CRYAB* in all patients. The mutation was inherited from their parents, who were heterozygous carriers of the variant showing no corresponding clinical manifestations. Additionally, the heterozygous mutation c.3G>A was also identified in multiple family members (Fig. 5). This mutation caused the loss of the initiating methionine and the functional α-B crystal protein (PVS1). The c.3G>A mutation frequency is relatively low in public databases (PM2), and the variation was predicted to be damaging by SIFT, Polyphen-2, and MutationTaster2 programs (PP3). Thus, this mutation was classified as pathogenic according to the standards of ACMG, which suggests that there is a high probability that the c.3G>A mutation is the cause of the fatal infantile hypertonic MFM.

4. Discussion

Infantile hypertonic MFM (OMIM 613869) is characterized by the early-onset of severe respiratory distress and hypertonic myopathy, mainly involving the trunk and neck muscles. This was first reported in several Canadian patients, and the pathology was named infantile hypertonic dystrophy at that time [2]. Muscular dystrophy usually first manifests as a weakness in the limbs; however, these individuals first experienced weakness in the trunk muscles. Thus, this disease was re-defined as a new type of early-onset MFM, and researchers suggested that it was a different disorder than a typical MFM or muscular dystrophy. So far, only limited cases have been reported, and the clinical diagnosis strategy is still unclear [1, 2]. Here, we analyzed four patients' clinical characteristics and summarized the disease features to improve the understanding of this disease and assist in diagnosing other cases.

The disease onset occurred at a few months old for all the infancy patients, which differs from typical MFM diseases since the onset usually occurred in adults [23]. All patients displayed a sudden onset of rigidity in their abdomen, neck, or back. In the early stage of the disease, we identified muscle lumps in 50% of patients, suggesting the fibrosis of affected myofiber. Additionally, we always observed abnormal sweat-
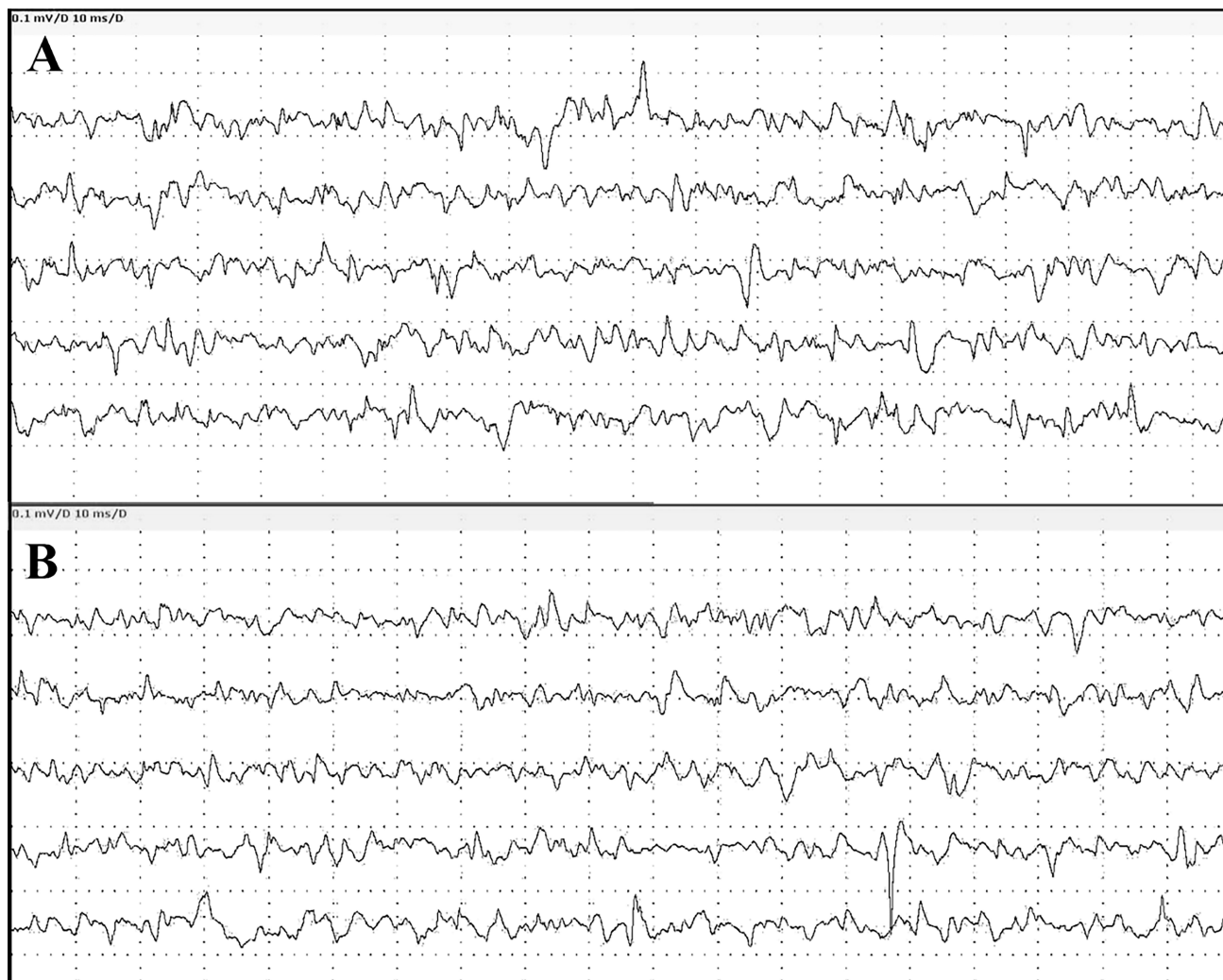
Fig. 3. Electromyograms (EMG) was performed in patient 1 (A) and patient 2 (B). Both patients presented with similar complex repetitive discharges (CRD), no waveform of myotonic discharge were identified.

ing, which may be due to the energy consumption caused by muscle rigidity and neurological dysfunction. We also noticed an acute progression of respiratory distress, which was probably caused by the rapid progression of endomysial fibrosis, especially in the *rectus abdominis*, which mainly supports infants' abdominal breathing [24]. The intercostal chest muscles that participate in the chest breathing of adolescents and elder children were also affected, which may also contribute to respiratory distress progression. The abnormal respiratory function affected the coughing and sputum excretion of patient 3. The pulmonary infection repeatedly occurred, leading to pulmonary hypertension and the right ventricular enlargement, which was detected by the electrocardiogram examination. What should be mentioned is that patients 2 and 4 showed an increase in anti-Acetylcholine (Ach) receptor antibodies in the serum. The elevated anti-Ach receptor antibodies were suspected to indicate MG [25].

However, the patient did not present with typical features of MG. So, the patient has not been diagnosed with MG; no

MG treatments have been given to the patients. The anti-Ach receptor antibodies have been reported to be detected in patients with muscular disorders, including myotonic dystrophy [26]. This could be coincidental. The presence of Ach receptor antibodies reflects the breaking of immune tolerance to Ach receptors due to autoinflammation secondary to muscle fiber degeneration [27]. However, the relationship between anti-Ach receptor antibody and these diseases have not been reported. We still could not explain the presence of Abs in a genetically diagnosed muscular myopathy.

Z-disk-related proteins such as desmin, B-crystallin, myotilin, ZASP, filamin C, and Bag3 are functionally affected by mutations in the MFM associated genes [26, 27]. *CRYAB* knockout mice develop kyphosis and myopathies involving mostly the posterior tongue and axial muscles but rarely the extremities [28]. Multiple MFM cases with *CRYAB* mutations have been reported, and it was identified as the genetic cause of MFM in both adults and infants [1, 27].
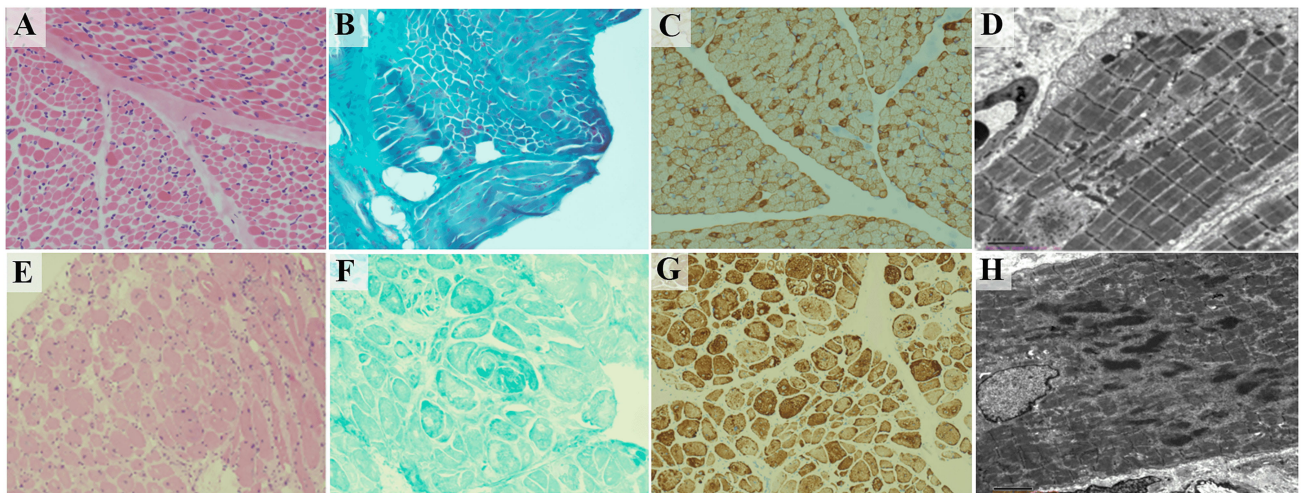
Fig. 4. Pathological changes in the vastus lateralis of patient 2 (four months and 20 days old, Fig. A-D) and rectus abdominis of patient 4 (six months old, Fig. E-H). (A) HE staining (100×) indicated clear boundaries between the muscle bundles, varying sizes of muscle fibers, and a small amount of degeneration or necrosis. (B) MGT staining (100×) showed varying sizes of abnormal red deposits in many muscle fibers. (C) Desmin staining (100×) was weak. (D) Electron microscopy identified most intact sarcomeres with a small amount of high-density deposits. (E) HE staining (200×) indicated unclear muscle bundle boundaries, varying size of muscle fibers, a large amount of necrosis, and different sizes of vacuoles. (F) MGT staining (200×) indicated the formation of vacuoles in the muscle fibers. (G) Desmin staining (200×) was strongly positive. (H) Electron microscopy identified damaged sarcomeres and a large amount of high-density deposits.
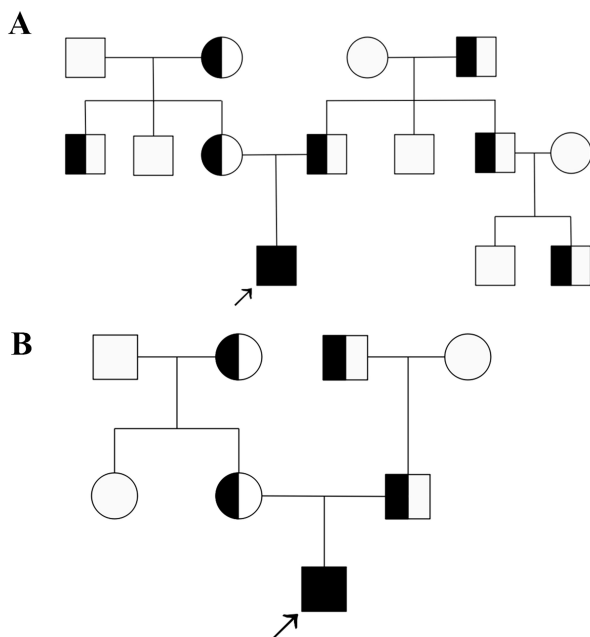

Fig. 5. Family pedigree of patient 2 (A) and patient 3 (B). Heterozygous mutation c.3G>A in the *CRYAB* gene was identified in the parents and multiple family members of these patients. Black symbols indicated affected patients with a homozygous mutation. White symbols showed healthy members with normal genotype. Half black and half white marks meant asymptomatic carriers with a heterozygous mutation. Arrows highlighted probands.

The c.3G>A mutation in *CRYAB* was detected in all four patients. This mutation affects the initiation of α-B crystal protein translation and causes a functional protein's loss of expression. A previous study indicated that the absence of α-B crystal protein or the presence of a mutant protein would increase the aggregation of desmin [29]. Our study showed a significantly increased accumulation of desmin and large aggregates in the patient's rectus abdominis myocytes. Additionally, we observed a severely disturbed sarcomere structure with muscle vesicles using an EM. The smearing of Z-disk and autophagic vacuoles, together with the accumulation of cytoplasmic filaments, indicated a fibrosis degeneration with phagocytosis and necrosis [30]. These histological images all presented a specific morphological change of MFM, which confirms the pathogenicity of the c.3G>A mutation in *CRYAB*.

Mutations in the *CRYAB* gene are also responsible for other autosomal dominant inheritance associated with multisystemic diseases such as cardiomyopathy, cataract genesis, and myopathic features [5, 7, 31, 32]. We observed an enlargement of the right ventricle in one of our patients, suggesting a possible cardiac function involvement. This was probably due to cardiac ischemia leading to sustained resting cardio muscle tension, as shown in murine models [33, 34]. However, we did not observe any cataract diseases among the affected patients.

It is interesting that all Canadian patients carry the same homozygous *CRYAB* mutation (c.60delC), while we identified the mutation c.3G>A in our 4 patients, as well as in another reported case of a Chinese infant with similar clinical manifestations [21]. This indicates that the hot spot mutation c.3G>A may be enriched in the Chinese population. The five Chinese patients are from the south of China, so we also speculated that the c.3G>A mutation could be a founder mu-

tation in this region. All the reported Chinese patients are male, which suggested males experiencing a more severe disease presentation and being thus more easily detected or less likely to be misdiagnosed. Further analyses, including more cases and complete family information, are required to validate these hypotheses.

Our study shows the homozygous mutation c.3G>A of *CRYAB* induced a fatal infantile hypertonic MFM. The patients were always born healthy but showed a disease onset early in infancy. In the early stage, the infants may present dysphagia, dyspnea, and hypertonia of the neck and trunk muscles mostly. The disease progressed rapidly, leading to irreversible respiratory failure, mild weakness of proximal limb muscles, vacuolization, muscle fiber necrosis, and poor prognosis. Muscle biopsies and genetic analysis could help in an earlier diagnosis. Then a better treatment might prevent the development of breathing difficulties and respiratory tract infections. We could also replace the defective gene in patients. Performing genome editing using various CRISPR/Cas-based therapeutics or providing a functional mRNA explicitly delivered to muscle cells provides an excellent potential for treating infantile hypertonic MFM in the foreseeable future [35, 36].

5. Conclusions

In this study, we reported 4 pediatric cases with symptoms similar to those of the fatal infantile hypertonic MFM with severe respiratory distress and a mutation in *CRYAB* reported in another Chinese patient [21]. Here, we speculate that the c.3G>A mutation is a possible hot spot mutation specific to the Chinese population. We also analyzed the clinical characteristics of our cases to improve the diagnosis of the disease. Further functional studies are required to confirm the clinical relevance of the c.3G>A mutation and the pathogenicity of the disease.

Abbreviations

αBC, Alpha B-crystallin; ALT, alanine aminotransferase; AST, aspartate aminotransferase; CK, creatine kinase; CKMB, creatine kinase myocardial bound; CRD, complex repetitive discharges; EM, electron microscopy; EMG, Electromyogram; IHC, immunohistochemistry; MFM, myofibrillar myopathy; MFM2, alpha-B crystallin-related myofibrillar myopathy (myofibrillar myopathy-2); MRI, magnetic resonance imaging.

Author contributions

CH designed and supervised the project and reviewed the manuscript. XL summarized the patient's information, reviewed the literature, and drafted the discussion of the manuscript. UY enrolled patients, arranged the clinical evaluation, and wrote the clinical portion of the manuscript. JM performed clinical tests. JL performed the biopsy staining and pathological assessment. YH analyzed the sequencing data, reviewed and revised the manuscript.

Conflict of interest

The authors declare that they have no competing interests.

References

[1] Odgerel Z, Sarkozy A , Lee HS, McKenna C, Rankin J, Straub V, *et al*. Inheritance pattern and phenotypic features of myofibrillar myopathy associated with BAG3 mutation. Neuromuscular Disorders. 2020; 20: 438-442.

[2] Lacson AG, Seshia SS, Sarnat HB, Anderson J, DeGroot WR, Chudley A, *et al*. Autosomal recessive, fatal infantile hypertonic muscular dystrophy among Canadian natives. The Canadian Journal of Neurological Sciences. 1995; 21: 203-212.

[3] Vicart P, Caron A, Guicheney P, Li Z, Prévost MC, Faure A, *et al*. A missense mutation in the alphaB-crystallin chaperone gene causes a desmin-related myopathy. Nature Genetics. 1998; 20: 92-95.

[4] Selcen D, Engel AG. Myofibrillar myopathy caused by novel dominant negative alpha B-crystallin mutations. Annals of Neurology. 2004; 54: 804-810.

[5] Sacconi S, Féasson L, Antoine JC, Pécheux C, Bernard R, Cobo AM, *et al*. A novel CRYAB mutation resulting in multisystemic disease. Neuromuscular Disorders. 2012; 22: 66-72.

[6] Mitzelfelt KA, Limphong P, Choi MJ, Kondrat FDL, Lai S, Kolander KD, *et al*. The human 343delT HSPB5 chaperone associated with early-onset skeletal myopathy causes defects in protein solubility. Journal of Biological Chemistry. 2016; 291: 14939-14953.

[7] Wójtowicz I, Jabłońska J, Zmojdzian M, Taghli-Lamallem O, Renaud Y, Junion G, *et al*. Drosophila small heat shock protein CryAB ensures structural integrity of developing muscles, and proper muscle and heart performance. Development. 2015; 142: 994-1005.

[8] Berry V, Francis P, Reddy MA, Collyer D, Vithana E, MacKay I, *et al*. Alpha-B crystallin gene (CRYAB) mutation causes dominant congenital posterior polar cataract in humans. American Journal of Human Genetics. 2001; 69: 1141-1145.

[9] Pilotto A, Marziliano N, Pasotti M, Grasso M, Costante AM, Arbustini E. alpha B-crystallin mutation in dilated cardiomyopathies: low prevalence in a consecutive series of 200 unrelated probands. Biochemical and Biophysical Research Communications. 2006; 346: 1115-1117.

[10] Liu Y, Zhang X, Luo L, Wu M, Zeng R, Cheng G, *et al*. A novel alpha B-crystallin mutation associated with autosomal dominant congenital lamellar cataract. Investigative Ophthalmology & Visual Science. 2006; 47: 1069-1075.

[11] Inagaki N, Hayashi T, Arimura T, Koga Y, Takahashi M, Shibata H, *et al*. Alpha B-crystallin mutation in dilated cardiomyopathy. Biochemical and Biophysical Research Communications. 2006; 342: 379-386.

[12] Devi RR, Yao W, Vijayalakshmi P, Sergeev YV, Sundaresan P, Hejtmancik JF. Crystallin gene mutations in Indian families with inherited pediatric cataract. Molecular Vision. 2008; 14: 1157-1170.

[13] Liu M, Ke T, Wang Z, Yang Q, Chang W, Jiang F, *et al*. Identification of a CRYAB mutation associated with autosomal dominant posterior polar cataract in a Chinese family. Investigative Ophthalmology & Visual Science. 2006; 47: 3461-3466.

[14] Chen Q, Ma J, Yan M, Mothobi ME, Liu Y, Zheng F. A novel mutation in CRYAB associated with autosomal dominant congenital nuclear cataract in a Chinese family. Molecular Vision. 2009; 15: 1359-1365.

[15] Safieh LA, Khan AO, Alkuraya FS. Identification of a novel CRYAB mutation associated with autosomal recessive juvenile cataract in a Saudi family. Molecular Vision. 2009; 15: 980-984.

[16] Reilich P, Schoser B, Schramm N, Krause S, Schessl J, Kress W, *et al*. The p.G154S mutation of the alpha-B crystallin gene (CRYAB) causes late-onset distal myopathy. Neuromuscular Disorders. 2010; 20: 255-259.

[17] Sun W, Xiao X, Li S, Guo X, Zhang Q. Mutation analysis of 12 genes in Chinese families with congenital cataracts. Molecular Vision. 2011; 17: 2197-2206.

[18] van der Smagt JJ, Vink A, Kirkels JH, Nelen M, ter Heide H, Molenschot MMC, *et al*. Congenital posterior pole cataract and adult onset dilating cardiomyopathy: expanding the phenotype of αB-crystallinopathies. Clinical Genetics. 2015; 85: 381-385.

[19] Xia X, Wu Q, An L, Li W, Li N, Li T, *et al*. A novel P20R mutation in the alpha-B crystallin gene causes autosomal dominant congenital posterior polar cataracts in a Chinese family. BMC Ophthalmology. 2015; 14: 108.

[20] Forrest KML, Al-Sarraj S, Sewry C, Buk S, Tan SV, Pitt M, *et al*. Infantile onset myofibrillar myopathy due to recessive CRYAB mutations. Neuromuscular Disorders. 2011; 21: 37-40.

[21] Ma K, Luo D, Tian T, Li N, He X, Rao C, *et al*. A novel homozygous initiation codon variant associated with infantile alpha-Bcrystallinopathy in a Chinese family. Molecular Genetics & Genomic Medicine. 2019; 7: e825.

[22] Richards S, Aziz N, Bale S, Bick D, Das S, Gastier-Foster J, *et al*. Standards and guidelines for the interpretation of sequence variants: a joint consensus recommendation of the American college of medical genetics and genomics and the association for molecular pathology. Genetics in Medicine. 2016; 17: 405-424.

[23] Fichna JP, Potulska-Chromik A, Miszta P, Redowicz MJ, Kaminska AM, Zekanowski C, *et al*. A novel dominant D109a CRYAB mutation in a family with myofibrillar myopathy affects αB-crystallin structure. BBA Clinical. 2017; 7: 1-7.

[24] Bellaye P, Wettstein G, Burgy O, Besnard V, Joannes A, Colas J, *et al*. The small heat-shock protein αB-crystallin is essential for the nuclear localization of Smad4: impact on pulmonary fibrosis. The Journal of Pathology. 2014; 232: 458-472.

[25] Somnier FE. Clinical implementation of anti-acetylcholine receptor antibodies. Journal of Neurology, Neurosurgery and Psychiatry. 1993; 56: 496-504.

[26] Lane RJ, Roncaroli F, Charles P, McGonagle DG, Orrell RW. Acetylcholine receptor antibodies in patients with genetic myopathies: clinical and biological significance. Neuromuscular disorders. 2012; 22: 122-128.

[27] Filippelli E, Barone S, Granata A, Nisticò R, Valentino P. A case of facioscapulohumeral muscular dystrophy and myasthenia gravis with positivity of anti-Ach receptor antibody: a fortuitous association? 2019; 40: 195-197.

[28] Carvalho AADS, Lacene E, Brochier G, Labasse C, Madelaine A, Silva VGD, *et al*. Genetic mutations and demographic, clinical, and morphological aspects of myofibrillar myopathy in a French cohort. Genetic Testing and Molecular Biomarkers. 2018; 22: 374-383.

[29] Fichna JP, Maruszak A, Żekanowski C. Myofibrillar myopathy in the genomic context. Journal of Applied Genetics. 2018; 59: 431-439.

[30] Batonnet-Pichon S, Behin A, Cabet E, Delort F, Vicart P, Lilienbaum A. Myofibrillar myopathies: new perspectives from animal models to potential therapeutic approaches. Journal of Neuromuscular Diseases. 2017; 4: 1-15.

[31] Elliott JL, Der Perng M, Prescott AR, Jansen KA, Koenderink GH, Quinlan RA. The specificity of the interaction between αB-crystallin and desmin filaments and its impact on filament aggregation and cell viability. Philosophical Transactions of the Royal Society of London. Series B, Biological Sciences. 2013; 368: 20120375.

[32] Bouhy D, Juneja M, Katona I, Holmgren A, Asselbergh B, De Winter V, *et al*. A knock-in/knock-out mouse model of HSPB8-associated distal hereditary motor neuropathy and myopathy reveals toxic gain-of-function of mutant Hspb8. Acta Neuropathologica. 2018; 135: 131-148.

[33] Jiaox X, Khan SY, Irum B, Khan AO, Wang Q, Kabir F, *et al*. Missense mutations in CRYAB are liable for recessive congenital cataracts. PLoS One. 2015; 10: e0137973.

[34] Li J, Horak KM, Su H, Sanbe A, Robbins J, Wang X. Enhancement of proteasomal function protects against cardiac proteinopathy and ischemia/reperfusion injury in mice. Journal of Clinical Investigation. 2011; 121: 3689-3700.

[35] Li C, Qiu Q, Wang Y, Li P, Xiao C, Wang H, *et al*. Time course label-free quantitative analysis of cardiac muscles of rats after myocardial infarction. Molecular BioSystems. 2014; 10: 505.

[36] Zhang L, Jian LL, Li JY, Jin X, Li LZ, Zhang YL, *et al*. Possible involvement of alpha B-crystallin in the cardioprotective effect of n-butanol extract of Potentilla anserina L. on myocardial ischemia/reperfusion injury in rat. Phytomedicine. 2019; 55: 320-329.

[37] Hung ME, Leonard JN. Stabilization of exosome-targeting peptides via engineered glycosylation. Journal of Biological Chemistry. 2015; 290: 8166-8172.

[38] Kim H, Yun N, Mun D, Kang JY, Lee SH, Park H, *et al*. Cardiac-specific delivery by cardiac tissue-targeting peptide-expressing exosomes. Biochemical and Biophysical Research Communications. 2018; 499: 803-808.